Since CF_2CH_2 is a near oblate top, $A \simeq B \simeq 2C$, the subband spacing in the perpendicular A_1 and B_1 bands is approximately equal to twice the line spacing in the ^PP and ^RR branches. Lines in the ^PP and ^RR branches of the pure rotation spectrum therefore superimpose to give a regular fine structure. Rotational transitions with $K_c = J$ contribute the greatest intensity to the observed lines. We have therefore labeled each multiple transition (in Table I) by the limiting value of $J = K_c$, e.g., $J = 15$, $K_c = 0$, $\nu = 11.259$ cm^{-1}, $J = 30$, $K_c = 30$, $\nu = 11.228$ cm^{-1}, i.e., 16 transitions lie within 0.031 cm^{-1}. The measurement accuracy of the observed transitions is insufficient to allow a more specific assignment than that just given. Some of the lines which possess easily identifiable patterns have not as yet been used as laser sources. However, by the application of low tuning fields it can be seen, as shown in Table II, that many more millimeter lines of known pure rotation transitions can be generated than by relying on chance coincidences. This type of electric field tuned laser action has recently been demonstrated by Fetterman *et al.* [9] using several lines of NH_3. Since much lower fields are required for CF_2CH_2 than for most of the NH_3 lines it is possible that, by a combination of the zero field lines that have already been observed with electric field produced lines, a very wide frequency coverage will be available using one gas CF_2CH_2.

TABLE I
ASSIGNMENT OF LASER LINES

CO_2 line	CO_2 λμm	Type of zero Field coincidence	Absorbing transition		CF_2H_2 laser emission λμm	CF_2CH_2 laser assignment	Ref
P12	10.5131	strong	$\nu_5 + \nu_{10}$	P(97)	288.5	$J = K_c = 96$	a
P12			ν_4	R(73)	375.0	$J = K_c = 73$	a
P12			ν_9	Q	884	$J = K_c = 30$	b
			ν_4	R	415	$J = K_c = 66$	b
P14	10.5321	weak	ν_4?	R	554.4	$J = K_c = 49$	a
			ν_9	Q	1020	$J = K_c = 26$	b
P22	10.6114	very strong	ν_9	P	890.0	$J = K_c = 30$	a
P22			ν_9	P	890.1	$J = K_c = 30$	a
P22			ν_9	P	990.0	$J = K_c = 27$	a
P24	10.6321	weak	ν_4	R	568.0	$J = K_c = 48$	b
P24			ν_9	P	663.3	$J = K_c = 41$	a
P30	10.6964	very strong	ν_9	P(61)	458.0	$J = K_c = 60$	a
R20	10.2466	weak	ν_9	R(59)	464.3	$J = K_c = 59$	a

[a] [1].
[b] [2].

TABLE II
ZERO FIELD COINCIDENCES AND POSSIBLE ZERO AND LOW ELECTRIC FIELD LASER TRANSITIONS

CO_2 line	CO_2 λμm	Type of zero field coincidence	Assigned low field line		Resonant field for pumping kV/cm	Possible laser transition J'-J"	Possible λmm
P_4	10.4406	medium					
P_6	10.4582	medium					
P_8	10.4762	strong	$^RQ_9$	ν_9	1.14	9 - 8	1.39
			$^RQ_6$	ν_9	3.33	6 - 5	1.96
P10	10.4945	strong	$^PQ_9$	ν_9	1.19	9 - 8	1.80
			$^PQ_{11}$	ν_9	2.14	11 - 10	1.44
			$^PQ_{13}$	ν_9	3.76	13 - 12	1.19
P20	10.5910	weak			zero		0.93
P36	10.7641	weak			zero		2.51
P38	10.7874	medium	$^SQ_9$	ν_4	1.16	9 - 8	1.39
P40	10.8111	medium	$^QQ_9$	ν_4	0.07	9 - 8	1.35

IV. CONCLUSIONS

The main conclusions that we have drawn from this study are the following.

1) That the lines observed have high J values, and in many cases the pump lines belong to the band whose center is furthest from the laser line.

2) That it should be possible using electric field tuning and less lossy cavities to observe many more strong laser lines in the 0.5–3-mm region.

REFERENCES

[1] S. F. Dyubko, V. A. Svich, and L. D. Fesenko, "Submillimeter-band gas laser pumped by a CO_2 laser," *JETP Lett.*, vol. 16, pp. 418–419, Dec. 1972.
[2] D. T. Hodges, R. D. Reel, and D. H. Barker, "Low-threshold CW submillimeter- and millimeter-wave laser action in CO_2-laser-pumped $C_2H_4F_2$, $C_2H_2F_2$ and CH_3OH," *IEEE J. Quantum Electron.* (Notes and Lines), vol. QE-9, pp. 1159–1160, Dec. 1973.
[3] S. M. Freund *et al.*, "Laser Stark spectroscopy in the 10 μm region: the ν_2 bands of CH_2F," *J. Mol. Spectrosc.*, to be published.
[4] J. W. C. Johns and A. R. W. McKellar, "Stark spectroscopy with the CO laser: The ν_2 fundamentals of H_2CO and D_2CO," *J. Mol. Spectrosc.*, vol. 48, pp. 354–371, Oct. 1973.
[5] F. Shimizu, "Stark spectroscopy of NH_3 ν_2 band by 10μ CO_2 and N_2O lasers," *J. Chem. Phys.*, vol. 52, pp. 3572–3576, Apr. 1970.
[6] D. R. Hall, Y. H. Pao, and P. C. Claspy, "Stark effect modulation of a passively Q-switched CO_2 laser," *Appl. Opt.*, vol 10, pp. 1688–1689, July 1971.
[7] D. R. Hall and Y.-H. Pao, "High-efficiency driven Q switching of the CO_2 laser using the Stark effect in molecular gases," *IEEE J. Quantum Electron.* (Corresp.), vol. QE-7, pp. 427–429, Aug. 1971.
[8] J. M. Martin, V. J. Corcoran, and W. T. Smith, "Identification of absorption lines in gases used to modulate the CO_2 laser," *IEEE J. Quantum Electron. (Special Issue on 1973 IEEE/OSA Conference on Laser Engineering and Applications, Part II of Two Parts)*, vol. QE-10, pp. 191–195, Feb. 1974.
[9] H. R. Fetterman, H. R. Schlossberg, and C. D. Parker, "C.W. submillimeter laser generation in optically pumped Stark tuned NH_3," *Appl. Phys. Lett.*, vol. 20, pp. 684–686, Dec. 1973.

Plasma Modulation of an HCN Gas Laser

G. D. TAIT, L. C. ROBINSON, AND D. V. BARTLETT

***Abstract*—A transient plasma is located within the Fabry–Perot resonator of a dc hydrogen cyanide laser. Plasma tuning sweeps the resonator modes through the emission line of the HCN molecules and produces pulses of far-infrared output radiation. Pulse production by hydrogen, nitrogen, helium, and argon pulsed plasmas is discussed.**

I. INTRODUCTION

The electrical discharge of a hydrogen cyanide gas laser produces molecules in a state of population inversion and, in addition, a plasma of positive ions and free electrons. When the discharge is pulsed the plasma electron density varies with time, its spatial distribution changes, and the nature of the laser radiation is markedly affected. In particular, "spikes" of submillimeter radiation can be produced [1].

In the experiment to be described in this short paper we have separated the effects of the transient plasma from the processes of HCN molecule formation and population inversion by using two physically separate discharges both located within the Fabry–Perot laser resonator. One is a dc discharge through a mixture of nitrogen and methane and the other is a pulsed discharge through a different gas.

Manuscript received June 5, 1974.
The authors are with the School of Physics, University of Sydney, Sydney, Australia.

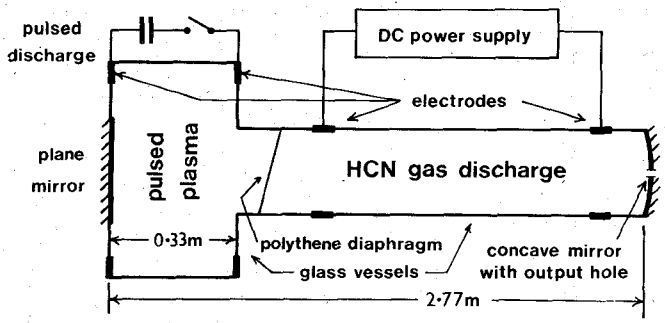

Fig. 1. Diagram of the laser-plasma system. Between the mirrors of a Fabry–Perot resonator we have a dc HCN laser discharge and an auxiliary pulsed discharge.

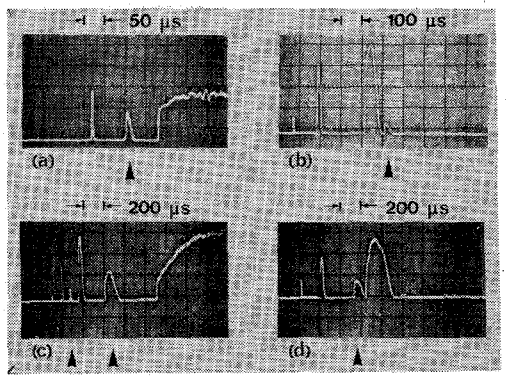

Fig. 2. Pulses of far-infrared radiation produced as resonances of a Fabry–Perot are swept by a decaying plasma through the emission lines of an HCN laser. The arrow-indicated lines are 311 μm and the others 337 μm. (a) Is for hydrogen and the trace starts at 100 μs. (b) Is nitrogen and the delay is 500 μs. (c) Is helium with delay 400 μs. (d) Is argon with initial delay 800 μs.

II. EXPERIMENTAL ARRANGEMENT

The experimental setup is shown in Fig. 1. The Fabry–Perot resonator has one plane mirror and one concave mirror with a radius of curvature of 3.7 m. They are separated by a distance of 2.77 m and laser radiation is coupled out through a 1.5-mm-diam hole in the curved mirror. This mirror is movable so the length of the resonator can be changed and the mirror alignment adjusted. Gases in the laser vessel are mixed in the ratio two parts methane to one part nitrogen and they flow at 0.5 l torr/s to give a pressure of 1 torr. This vessel has a diameter of 7.5 cm and it is excited by a 1-A continuous-discharge current. The pulsed-discharge vessel has a 25-cm diameter and a length of 33 cm. It is attached to the end of the laser-discharge vessel but the two discharges are separated by a polyethylene diaphragm 100 μm thick. We have used the following gases in this auxiliary-discharge vessel: hydrogen, helium, nitrogen, and argon. Pressures have been typically 20 m torr, and the excitation voltage 20 kV. Ionization is produced by the discharge of a 1-μF capacitor connected via an ignitron switch. After the short high-current pulse the electron density decays; the rate of decay is different for the various gases used, hydrogen being the fastest and argon and helium the slowest.

Pulses of output radiation are generated as the decaying electron density of the pulsed plasma sweeps the resonant frequencies of the Fabry–Perot through the HCN emission line. These pulses are detected with a free-carrier photoconductive detector with a submicrosecond response time and they are displayed on an oscilloscope.

III. PULSE PRODUCTION BY TRANSIENT HYDROGEN, NITROGEN, HELIUM, AND ARGON PLASMAS

Fig. 2 shows pulses generated by resonator mode sweeping by hydrogen, nitrogen, helium, and argon plasmas. In Fig. 2(a) hydrogen decay results in the onset of three pulses of radiation between the times 260 and 430 μs after breakdown. Two of these pulses are 337-μm radiation and one is 311 μm. With nitrogen plasma in Fig. 2(b) we have four pulses arising at times between 620 and 1005 μs. Helium plasma shows six pulses in Fig. 2(c) with onset times between 700 μs and 1.7 ms, while argon shows in Fig. 2(d) four pulses starting at times between 1 and 1.64 ms after breakdown.

By moving one of the Fabry–Perot mirrors by means of a micrometer one can change the length of the resonator in small steps. The plasma refractive index at 337 μm is

$$[1 - n(t)/N]^{1/2}$$

where $n(t)$ is the time-dependent electron density and $N = 9.8 \times 10^{15}$ cm^{-3}; as $n(t)$ decreases it can increase the effective resonator length. Thus, if we mechanically lengthen the resonator, the onset of a given pulse will be earlier in time. This effect is shown in Fig. 3. Here the Fabry–Perot mirror separation has been increased in successive steps of 20 μm. By such a plot a particular pulse can be traced through mirror displacements of several wavelengths and the repeat interval of the curves can give us the half wavelength of the pulse of radiation. We have thus identified the pulses of 337- and 311-μm radiation indicated in Fig. 2.

As the resonator length is changed the number, and to some extent the shape, of pulses changes. Thus, for example, we obtain the output of Fig. 4 by decreasing the resonator length of Fig. 2(d) by 100 μm. The four pulses of Fig. 2(d) now start at times between 940 μs and 1.1 ms, and new pulses arise late in the decay. The new pulses overlap at 2.23 ms and are associated with overlapping modes of the resonator.

By following a pulse of output radiation from late in the plasma decay when the density $n(t)$ is negligibly small—for example, at the beginning of the plateau of output at time 470 μs in Fig. 2(a) we can assign $n(t)$ a zero value—we can plot the density as a function of time by noting that for p successive 20-μm mirror displacements the effective plasma density has increased by $n(t)$, where

$$\{[1 - n(t)/N]^{1/2} - 1\}L$$

is equal to $(20p)$ μm. Here L is the length of the plasma. We can

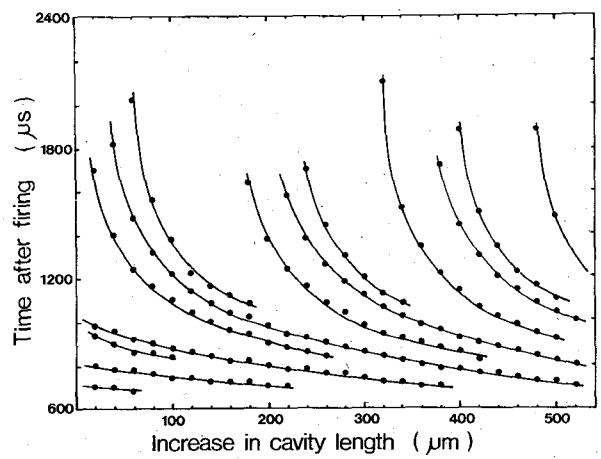

Fig. 3. Plot showing the time of onset of plasma-produced laser pulses as a function of laser mirror separation. The repeat interval of the curves is equal to half of the wavelength of the radiation.

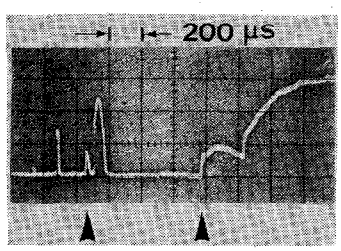

Fig. 4. Pulses produced with an argon plasma. This oscilloscope trace should be compared with Fig. 2(d) which was obtained under similar conditions except that in this figure the mirror separation is 100 μm greater.

also measure densities by means of microwave interferometry [2].

Laser pulses arise during the decay of the plasma and not during breakdown. In general the plasma density rises to a peak value above 10^{14} cm^{-3}, but the onset of laser pulsing occurs only for $n \simeq 3 \times 10^{13}$ cm^{-3}. There are two possible reasons why pulses do not occur at higher densities: the collision frequency in the plasma may be sufficiently high at early times to keep the laser below its oscillation threshold; alternatively the radial plasma-density profile may cause enough beam refraction to prohibit the buildup of oscillations.

Because the plasma electron density is higher on the laser axis than at the outside of the laser beam, the plasma acts as a diverging element in the cavity and can render the cavity unstable. The effect of refraction can be calculated from a simple modification of well-known theory [3]. It has been shown that in conventional pulsed lasers, beam refractive effects of the plasma may well limit the earliest time at which laser pulses can be obtained [4], [3]. To avoid this limitation in the present experiment, we have taken the following steps. First, a resonator design is chosen with the strongest possible converging mirror consistent with reliable CW operation. Secondly, a short high-density plasma is used, since a greater length change can be obtained while maintaining resonator stability than with the comparatively long low-density plasma of a conventional pulsed laser. Finally, a large-diameter plasma vessel is employed. As a result the cavity should remain stable for electron densities up to about 5×10^{14} cm^{-3}.

A small-diameter discharge vessel would give a steep radial density profile which significantly limits the earliest times of pulse onset. For example, if the auxiliary discharge-vessel diameter is reduced to that of the laser (7.5 cm) the stability limit would be 5×10^{13} cm^{-3}. In our previous studies of spiking we used a pulsed HCN laser of a diameter 7.5 cm with similar length and mirror configuration. The plasma in this case occupied most of the length of the resonator and resulted in a further reduced stability limit of 3×10^{12} cm^{-3}. The onset of spiking did in fact occur at about this density [1], [4].

While the shorter pulsed plasma vessel has reduced beam refraction, the plasma density must be higher. This has introduced another limitation on pulse onset time. The laser radiation intensity is attenuated in passing through the plasma as a result of collisional damping by a factor of

$$\exp(-4\pi m\nu/\omega)$$

per pass, where m is the length change in radiation wavelengths due to the plasma, ν is the plasma-electron collision frequency, and ω is the radiation angular frequency. The collision frequency varies as the plasma density and hence for a given length change (m constant) greater attenuation occurs if a short high-density plasma is used.

From observations of attenuation of microwaves of frequency 120 GHz we have estimated the collisional frequency and thence the loss per pass of the laser beam. The collision frequency is about 10^{10} s^{-1} at the time of onset of laser pulses and the loss per pass of the laser beam is between 2 and 3 percent for all gases used. At the times of the last pulses collisional losses are negligibly small. Collisions give the largest time-dependent loss process in our system and it appears that this is the factor limiting the earliest times at which pulses are produced by the laser.

TABLE I
PULSEWIDTHS

onset time (μs)	base width (μm)
480	10
520	17
590	25
660	29
750	32
890	34

IV. COMMENTS ON PULSEWIDTHS, AND THE FEASIBILITY OF PLASMA Q SWITCHING

Our studies of the shapes of the emitted pulses are at an early stage, but some preliminary data may be of interest.

Some widths of pulses produced by nitrogen plasma are given in Table I. They express the width at the base of the pulses in terms of equivalent length changes of the resonator. The shortest pulses last about 5 μs.

We find that, in general, the pulses are asymmetric in shape and they tend to be narrower than the HCN-laser gainwidth. At early times we observe widths of 10 μm, but at late times when the plasma sweeps the resonance slowly through the laser gain curve the widths are about equal to the gainwidth.

It is clear from the oscilloscope traces shown in Fig. 2 that there are two regions of buildup of a pulse. A rapid rise precedes a more gradual change in output. This indicates that lasing starts within the gain curve of the laser and thereafter follows the gain curve. Although it is not clear from Fig. 2 we find that the plasma sweeps the resonance closer to line center before buildup occurs in the earlier pulses, and even beyond line center in the earliest pulses. This suggests that our plasma sweeping is sufficiently fast for Q switching. However, we observe no power enhancement with this form of Q switching. This is consistent with the observations of other workers using conventional techniques and it suggests that the upper laser level is too short-lived to give output enhancement.

The fact that plasma sweeping at early times can be so fast as to take the resonance beyond line center before output buildup suggests a third mechanism which can limit the earliest onset times of pulses. We have thus far ascribed pulse-onset limitations to collisional damping, for this is significant at the earliest times. Our present experiments are, however, being directed towards the distinguishing of these effects.

REFERENCES

[1] L. B. Whitbourn, L. C. Robinson, and G. D. Tait, "The origin of spiking pulses in HCN gas lasers," *Phys. Lett. A*, vol. 38, pp. 315–317, Feb. 28, 1972.
[2] G. D. Tait, L. B. Whitbourn, and L. C. Robinson, "Short pulses from a plasma controlled HCN gas laser," *Phys. Lett. A*, vol 46, pp. 239–240, Dec. 1973.
[3] B. W. McCaul, "Plasma self Q-switching in far-infrared lasers," *Appl. Opt.*, vol. 9, pp. 653–663, Mar. 1970.
[4] L. B. Whitbourn, "The propagation of electromagnetic waves in laboratory plasmas," Ph. D. dissertation, Sydney University, Sydney, Australia, 1973.